Appl. Phys. B 72, 641–645 (2001) / Digital Object Identifier (DOI) 10.1007/s003400100547

Applied Physics B
Lasers
and Optics

Influence of optical-damage-resistant dopants on the nonlinear optical properties of lithium niobate

D. Xue*, **K. Betzler****

Fachbereich Physik, Universität Osnabrück, 49069 Osnabrück, Germany

Received: 24 October 2000/Published online: 21 March 2001 –

Abstract. Using the chemical-bond method, nonlinear optical properties of lithium niobate containing different dopants are calculated. In crystals with stoichiometric composition the second order nonlinear susceptibility decreases approximately linearly with increasing dopant concentration. Among the dopants studied – Mg, Zn and In – this behaviour is most highly expressed for In doping. In contrast to that, congruently grown crystals show a different behaviour; only a weak dependence on the dopant concentration is found for, for example, Mg-doped material.

PACS: 42.65.Ky; 77.22.Ch; 77.84.Dy

Due to an attractive combination of piezoelectric, electro-optical, and – linear and nonlinear – optical properties [1, 2], lithium niobate ($LiNbO_3$) is one of the most interesting inorganic materials for a wide range of applications. Optical devices fabricated from $LiNbO_3$ include holographic memories, optical demultiplexers, photorefractive devices, waveguide structures, electro-optic modulators, solid-state lasers, frequency doublers and mixers, and parametric oscillators. Unfortunately, many of these optical applications are hampered by the so-called optical damage – optically induced refractive-index inhomogeneities in the material [3]. Such refractive-index changes show up when crystals are exposed to visible light, even at moderate light intensities, due to the photorefractive effect.

Optical damage is known be greatly reduced by damage resistant ions when co-doping $LiNbO_3$ crystals with MgO [4, 5], ZnO [6], or In_2O_3 [7]. This is due to the influence of Mg^{2+}, Zn^{2+}, or In^{3+} ions on the intrinsic defect structure [7–9] of lithium niobate (for a recent review read [10], which includes an extensive bibliography). Yet these dopants affect not only the photorefractive but also nearly all other optical properties of lithium niobate. Their influence on the linear susceptibility has recently been studied in great detail investigating the absorption edge [11] or the refractive indices [12–16], which sensitively define the phase-matching conditions for different configurations of nonlinear optical processes such as second harmonic generation (SHG) or wave mixing.

In the present work a comparison of the dopant influences on the nonlinear optical response, i.e., the SHG susceptibility tensor, of lithium niobate is presented. Linear and nonlinear susceptibilities are calculated applying the chemical-bond viewpoint [17–19]; the influence of the dopants on the dielectric response is quantitatively analyzed on the basis of a simplified structural description of lithium niobate.

1 Theoretical method

As shown in previous works (for an overview see [17]), the chemical-bond method regards certain macroscopic physical properties of a crystal as the combination of the contributions of all constituent chemical bonds. A multibond crystal $A_aB_b \ldots$ is split up into constituent bonds A–B with appropriately chosen partial charges which can be deduced from the detailed chemical-bonding structures of atoms A and B in the crystal. The distribution of the valence electrons of constituent atoms over the contributing bonds is defined by the bond-valence equation, which is derived from the bond graph of the compound (see Sect. 2).

To obtain the (isotropic) linear susceptibility of a crystal material, the contributions of all individual scalar linear bond susceptibilities have to be summed up. To obtain the nonlinear susceptibility, the individual tensorial nonlinear bond susceptibilities have to be summed up geometrically. The results thus automatically obey the symmetry rules for third rank tensors and, moreover, the so-called Kleinman symmetry rule [20].

The macroscopic linear susceptibility of a crystal is given by the sum over all contributions and can be written as

$$\chi = \sum_{\mu} F^{\mu} \chi^{\mu} = \sum_{\mu} N_{\mathrm{b}}^{\mu} \chi_{\mathrm{b}}^{\mu} \tag{1}$$

Present address: Department of Chemistry, University of Ottawa, Ottawa, Canada
**Corresponding author.
(Fax: +49-541/9691-2636, E-mail: klaus.betzler@uni-osnabrueck.de)

with

F^μ: Fraction of bonds of type μ composing the crystal.
χ^μ: Linear susceptibility contribution from bonds of type
N_b^μ: Number of bonds of type μ per cm^3.
χ_b^μ: Susceptibility of a single bond of type μ.

According to Phillips [21] and Van Vechten [22], the linear susceptibility χ^μ contributed by the bonds of type μ in a crystal can be defined as

$$\chi^\mu = (4\pi)^{-1}(\hbar\Omega_p^\mu / E_g^\mu)^2 , \tag{2}$$

where Ω_p^μ is the plasma frequency and E_g^μ is the average energy gap between the bonding and antibonding states of the bond. E_g^μ can be separated into homopolar and heteropolar (i.e., covalent and ionic) contributions E_h^μ and C^μ

$$(E_g^\mu)^2 = (E_h^\mu)^2 + (C^\mu)^2 , \tag{3}$$

$$E_h^\mu = K_1/(d^\mu)^{2.48} , \tag{4}$$

$$C^\mu = K_2 b^\mu \exp(-k_s^\mu r_0^\mu)\left[(Z_A^\mu)^* - n(Z_B^\mu)^*\right] r_0^\mu , \tag{5}$$

where K_1 and K_2 are constants consisting only of physical fundamental constants such as $\hbar, e, \ldots$ and adapted to the units of measure used in the concrete calculation (for lengths in Å and energies in eV, the numerical values are $K_1 = 39.74$ and $K_2 = 14.4$ [23]). $d^\mu = 2r_0^\mu$ is the bond length of the μ-type bond A–B, $\exp(-k_s^\mu r_0^\mu)$ is the Thomas–Fermi screening factor. $(Z_A^\mu)^*$ and $(Z_B^\mu)^*$ are the effective numbers of valence electrons of the two atoms in the bond, and n is the ratio of the numbers of the two elements B and A in the bond-valence equation [24]. Because the true screening behaviour in a solid is more complex than this simple Thomas–Fermi description, a correction factor b^μ is introduced [22]. This factor is also used to correct for d-electron influences not accounted for in the effective Z^*. These d-electron effects on the bond susceptibilities were first considered by Levine [23] but are still subject to discussion [25, 26]. According to Levine [27], the different factors b^μ can be written as $b^\mu = \beta(\bar{N}_c^\mu)^2$, with one global parameter, β (global for all different bonds in the compound), where $\bar{N}_c^\mu$ is the average coordination number of the ions A and B in the bond μ. If the linear susceptibility, i.e., the refractive index, of a crystal is known, β can be adjusted to describe the linear susceptibility exactly. Thus, in general, also the results for the nonlinear susceptibility are improved.

The description of the second-order nonlinear susceptibility can be derived in a similar way; this was basically done by Levine [28], and extensions for complex crystals were developed by Xue and Zhang [17]. The final result for the second-order nonlinear optical tensor coefficients d_{ij} can be written as the appropriate geometric sum over the contributions of all constituent bonds:

$$d_{ij} = \sum_\mu \frac{G_{ij}^\mu N_b^\mu (\chi_b^\mu)^2}{d^\mu q^\mu} \left\{ \frac{f_i^\mu \left[(Z_A^\mu)^* + n(Z_B^\mu)^*\right]}{2\left[(Z_A^\mu)^* - n(Z_B^\mu)^*\right]} + \frac{s(2s-1)(r_0^\mu)^2 f_c^\mu \varrho^\mu}{(r_0^\mu - r_c^\mu)^2} \right\} . \tag{6}$$

The first part denotes the ionic fraction, the second part the covalent fraction of the nonlinear optical coefficient. The constants on the right side of (6) are as follows:

G_{ij}^μ: Geometrical contribution of chemical bonds of type μ.
N_b^μ: Number of bonds of type μ per cm^3.
χ_b^μ: Susceptibility of a single bond of type μ.
$(Z_A^\mu)^*$, $(Z_B^\mu)^*$: Effective number of valence electrons of A and B ions, respectively.
n: Ratio of numbers of two elements B and A in the bond bond valence equation [24].
f_i^μ, f_c^μ: Fractions of ionic and covalent characteristics of the individual bonds [see (3)], $f_i^\mu = (C^\mu)^2/(E_g^\mu)^2$ and $f_c^\mu = (E_h^\mu)^2/(E_g^\mu)^2$.
d^μ: Bond length of the μ type bonds in Å.
q^μ: Bond charge of the μth bond.
s: Exponent in the bond force constant (2.48).
$r_c^\mu = 0.35 r_0^\mu$: Core radius, where $r_0^\mu = d^\mu/2$.
$\varrho = (r_A^\mu - r_B^\mu)/(r_A^\mu + r_B^\mu)$: Difference in the atomic sizes, r_A^μ and r_B^μ are the covalent radii of atoms A and B.

All of the above constants have to be deduced from a structural analysis based on the crystallographic structure, taking into account the detailed chemical bonding situation of all constituent atoms [17]. It should be emphasized that besides the parameter β introduced for the linear susceptibility no further adjustable parameters are included.

2 Structural analysis

In pure lithium niobate of stoichiometric composition, the ideal cation stacking sequence along the polar c axis of the crystal can be described by $\ldots - \mathrm{Li} - \mathrm{Nb} - \square - \mathrm{Li} - \mathrm{Nb} - \square - \ldots$, where $\square$ represents a structural vacancy (an empty oxygen octahedron) [29]. This crystal structure is illustrated in Fig. 1. The structural situation changes when dopants are introduced into the crystallographic frame of pure lithium niobate. Nearly all two- or three-valenced dopants are found to occupy Li sites [30, 31] – at least at low doping levels (up to a few percent). Charge compensation is accomplished by the formation of an appropriate number of Li vacancies. As

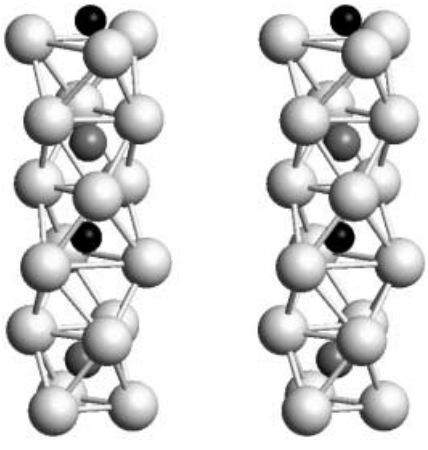

Fig. 1. Stereoscopic view (to be viewed with crossed eyes) of the ideal crystal stacking sequence of lithium niobate along the crystallographic c-axis (*light gray*: oxygen, *dark gray*: niobium, *black*: lithium). The *sticks* sketch the slightly distorted oxygen octahedra mutually connected via triangular faces

illustrated in Fig. 2, this modifies the local chemical-bonding state in the crystal, especially for the oxygen atoms around the dopants and the vacancies, in a more or less random way. As an exact numerical treatment of such a disturbed crystal is not possible to date, one has to introduce some practical simplifications.

The chemical-bond method [17–19] treats a compound as an infinite network of constituent atoms linked by chemical bonds. For pure crystals, this can be reduced to a finite network comprising a single formula unit such as the network of $LiNbO_3$, in which Li^+ and Nb^{5+} are six-coordinated (with O^{2-} anions) and O^{2-} is four-coordinated (with two Li^+ cations and two Nb^{5+} cations). The detailed chemical-bonding description for pure $LiNbO_3$ is shown in Fig. 3. In such graphs, each line represents a different bond, and each atom A in the corresponding lattice is assigned a formal charge equal to its atomic valence or oxidation state (V_A) and each bond between atoms A and B is assigned a bond valence (s_{AB}). The sum of the bond valences (each with appropriate algebraic sign according to the bond direction) at each node atom in the network equals its formal charge, the sum around any loop is zero [18, 19]:

$$\sum_{B} s_{AB} = V_A, \qquad \text{and} \qquad \sum_{\text{loop}} s_{AB} = 0\,. \tag{7}$$

Calculations of the crystal susceptibility are based on such a suitable decomposition of the crystal into single bonds.

The exact treatment of doped lithium niobate would require a large number of such bond graphs, each describing one of the possible environments around a dopant ion (Fig. 2 shows one of the possible arrangements). To avoid such complications with randomly distributed modified bonding situations, we treat doped lithium niobate instead as an appropriate mixture of pure lithium niobate with pure "metal" niobate (metal = Mg, Zn, In, ...). Of course, this approximative approach cannot be used in general, albeit that it can be successfully applied for the calculation of optical properties. This is due to the fact that optical wavelengths are rather large compared to typical interatomic distances; a summation over a fixed distribution of small regions will yield the same optical susceptibility as a summation over a random distribution. Consequently, for the description and decomposition of doped lithium niobate, we use the bond graphs of the metal niobates $M^{II}Nb_2O_6$ and $M^{III}Nb_3O_9$ (M^{II} = Mg, Zn; M^{III} = In) in addition to that of pure lithium niobate (Fig. 3). For $M^{III}Nb_3O_9$, this graph is sketched in Fig. 4.

Thus crystals of doped lithium niobate $Li_{1-x}M^{II}_{x/2}NbO_3$ and $Li_{1-x}M^{III}_{x/3}NbO_3$ are formally treated as $(1-x)\cdot LiNbO_3 + \frac{x}{2}\cdot M^{II}Nb_2O_6$ and $(1-x)\cdot LiNbO_3 + \frac{x}{3}\cdot M^{III}Nb_3O_9$, respectively. As a further approximation in the calculations, the geometrical structure data for the metal niobates are adopted from pure lithium niobate. Generally, it must be assumed that the crystal lattice would relax its geometry slightly around dopants and vacancies due to the altered ionic charges. Yet, to date no experimental structural data are available which describe the relaxed lattice around impurities in lithium niobate correctly.

Lithium niobate is usually grown in the congruently melting composition, exhibiting a lithium deficit of approximately 1.5%. Various defect structure models have been proposed for this case [29, 32, 33]. The newer results [33] prove that only Nb antisite defects and Li vacancies exist. Thus the dielectric properties of such nonstoichiometric crystals can be structurally treated in exactly the same manner as discussed above for doped stoichiometric material.

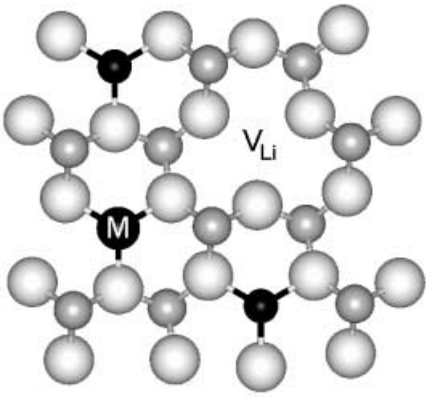

Fig. 2. Chemical bonds in lithium niobate. Sketched is one oxygen plane perpendicular to the crystallographic *c*-axis and the adjacent Li and Nb sites (*light gray*: oxygen, *dark gray*: niobium, *black*: lithium). Li sites below the oxygen plane are hidden by the corresponding Nb ions above the plane. M denotes a dopant occupying a Li site, V_{Li} a lithium vacancy

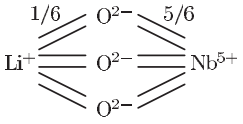

Fig. 3. Bond graph of lithium niobate. Each *line* represents a structurally different bond; formal charges of the bonds and ions are indicated

3 Results and discussion

The linear and nonlinear susceptibilities of doped stoichiometric and Mg-doped congruent lithium niobate are found for a wavelength of 1064 nm (Nd:YAG laser) according to the schemes outlined in the previous two sections. Through a structural analysis the crystals are partitioned into constituent bonds, and the individual bond susceptibilities are calculated. The macroscopic properties are computed via appropriate scalar or geometric sums. The fit parameter β discussed in Sect. 1 is derived from a comparison of the macroscopic linear susceptibility with refractive-index values [12–16] for each of the dopants, and further on it is used for the nonlinear susceptibilities.

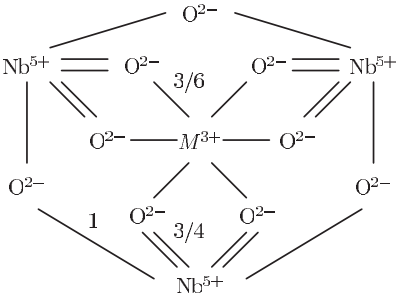

Fig. 4. Bond graph of $M^{III}Nb_3O_9$ (M^{III} denotes a three-valenced cation, e.g., In or Sc). The formal charges of the bonds and ions are indicated

3.1 Stoichiometric lithium niobate

The detailed results for the bond susceptibilities have been presented in previous publications for stoichiometric lithium niobate with Mg [34], Zn [35], and In [36] doping. Therefore, here only the final results for the nonlinear susceptibilities are summarized in Fig. 5. All tensor coefficients d_{ij} decrease with increasing dopant concentration; the behaviour for Mg and Zn doping is very similar, for In doping the decrease is expressed considerably more.

Our calculated results for pure lithium niobate are $d_{22} = 2.71\,\mathrm{pm/V}$, $d_{31} = 4.13\,\mathrm{pm/V}$ and $d_{33} = 22.9\,\mathrm{pm/V}$, values which agree well with the reported experimental data given by Roberts [37] (adopted from Miller et al. [38]) – $d_{22} = 2.1\,\mathrm{pm/V}$, $d_{31} = 4.3\,\mathrm{pm/V}$ and $d_{33} = 27\,\mathrm{pm/V}$ – and by Shoji et al. [39] – $d_{31} = 4.6\,\mathrm{pm/V}$ and $d_{33} = 25.2\,\mathrm{pm/V}$ (for d_{31} and d_{33} – which have negative signs – here and in the figures absolute values are given).

The dependencies of the coefficients d_{ij} of doped lithium niobate on the dopant concentration can be summarized as follows:

$$d_{22} = 2.71\cdot(1 - 0.026\,c_{\mathrm{Mg}} - 0.023\,c_{\mathrm{Zn}} - 0.064\,c_{\mathrm{In}}), \quad (8)$$

$$d_{31} = 4.12\cdot(1 - 0.028\,c_{\mathrm{Mg}} - 0.026\,c_{\mathrm{Zn}} - 0.097\,c_{\mathrm{In}}), \quad (9)$$

$$d_{33} = 22.9\cdot(1 - 0.027\,c_{\mathrm{Mg}} - 0.024\,c_{\mathrm{Zn}} - 0.082\,c_{\mathrm{In}}), \quad (10)$$

where d is in pm/V and c is the molar percentage of the respective oxide (MgO, ZnO, In_2O_3).

The decrease in the nonlinear susceptibility with increasing doping level indicates that the dopants directly or indirectly reduce the acentricity of the material. The reason for the more highly expressed decrease for In doping may be the scaling used. The "molar" impurity concentration is usually related to the basic oxides composing the material. These basic oxides are Li_2O, Nb_2O_5, MgO, ZnO, and In_2O_3, respectively. Taking this and the respective valence state into account, In_2O_3 introduces four times as many Li vacancies as MgO or ZnO into the crystallographic frame of lithium niobate. The ratio of the respective slopes in Fig. 5 is also approximately four. Thus the number of Li vacancies connected with the dopants seems to be mainly responsible for the decrease found, fairly independent of the specific impurity used.

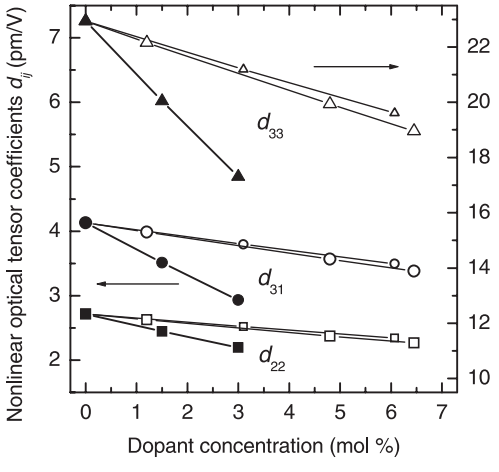

Fig. 5. Calculated nonlinear optical tensor coefficients d_{ij} for stoichiometric lithium niobate with various dopants as a function of the dopant concentration. *Solid markers*: In-doped, *small open markers*: Zn-doped, *large open markers*: Mg-doped lithium niobate

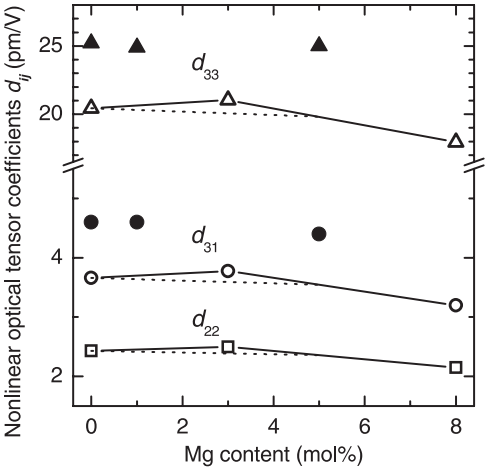

Fig. 6. Nonlinear optical tensor coefficients d_{ij} for Mg-doped congruently grown lithium niobate as a function of the Mg content. *Solid lines* are calculated according to the "ideal" structural scheme proposed by Iyi et al. [40], *dashed lines* correspond to their "real" measured data and *solid symbols* represent experimental data measured by Shoji et al. [39]

3.2 Congruent lithium niobate

The calculations for Mg-doped congruent lithium niobate are based on the structural data derived by Iyi et al. from a combination of chemical analysis, lattice parameter measurements and density measurements [40]. Using their data and following the structural analysis discussed in the previous section, an appropriate combination of two components, Li-deficient and Mg-doped material, is used to compute the susceptibilities. The individual bond susceptibility data for the various constituent bonds of the two components are adopted from previous detailed calculations [24, 34].

Our results – together with the available experimental data [39] – are summarized in Fig. 6. In contrast to stoichiometric lithium niobate, we find only a relatively weak dependence on the dopant concentration in congruent material. The tendency for the calculated results is the same as for the experimental data also shown in Fig. 6, which are also nearly independent of the Mg content. This behaviour is in very good agreement with our model proposed above, which assumes that the doping dependence of the nonlinear susceptibility is primarily determined by the concentration of the Li vacancies, not by the concentration and type of dopants. According to the measurements of Iyi et al. [40] and their proposed structural model, this concentration of Li vacancies is approximately constant for Mg-doping levels up to about 5 mol% in congruently grown lithium niobate.

4 Conclusion

Second-order nonlinear optical properties of stoichiometric lithium niobate doped with various dopants and Mg-doped congruent lithium niobate have been quantitatively studied from the chemical-bond viewpoint of crystal materials. Substituting two- or three-valenced cations for Li ions in stoichiometric crystals decreases the second-order nonlinear optical

response of lithium niobate, more strongly for three-valenced than for two-valenced ions. In congruently grown crystals, the nonlinear susceptibility is nearly independent of the doping level, at least at low concentrations. Both the expressed dopant-specific linear dependence on the dopant concentration in stoichiometric crystals and the approximate independence in congruent crystals can be explained in a unified model if one assumes that variations in the nonlinear susceptibility mainly depend on the concentration of lithium vacancies. This dependence is linear in a very good approximation.

Acknowledgements. D. Xue thanks the Alexander von Humboldt Foundation for all support during his stay in Germany.

References

1. A. Räuber: In *Current Topics in Materials Sciences*, ed. by E. Kaldis (North Holland, Amsterdam 1978) p. 481
2. E. Krätzig, O.F. Schirmer: In *Photorefractive Materials and Their Applications*, ed. by P. Günter, J.P. Huignard (Springer, Berlin, Heidelberg 1988) p. 131
3. A. Ashkin, G.D. Boyd, J.M. Dziedzic, R.G. Smith, A.A. Ballman, J.J. Levinstein, K. Nassau: Appl. Phys. Lett. **9**, 72 (1966)
4. G. Zhong, J. Jin, Z. Wu: In Proceedings of the 11th International Quantum Electronics (Institute of Electrical and Electronics Engineers, New York 1980) p. 631
5. K. Niwa, Y. Furukawa, S. Takekawa, K. Kitamura: J. Cryst. Growth **208**, 493 (2000)
6. T.R. Volk, V.J. Pryalkin, N.M. Rubinina: Opt. Lett. **15**, 997 (1990)
7. T.R. Volk, N.M. Rubinina: Ferroelectr. Lett. **14**, 37 (1992)
8. T. Volk, M. Wöhlecke, N. Rubinina, A. Reichert, N. Razumovski: Ferroelectrics **183**, 291 (1996)
9. T. Volk, M. Wöhlecke, N. Rubinina, N.V. Razumovski, F. Jermann, C. Fischer, R. Böwer: Appl. Phys. A **60**, 217 (1995)
10. T.R. Volk, M. Wöhlecke: Ferroelectrics Review **1**, 195 (1998)
11. J.J. Xu, G.Y. Zhang, F.F. Li, X.Z. Zhang, Q.A. Sun, S.M. Liu, F. Song, Y.F. Kong, X.J. Chen, H.J. Qiao, J.H. Yao, L.J. Zhao: Opt. Lett. **25**, 129 (2000)
12. U. Schlarb, K. Betzler: Phys. Rev. B **50**, 751 (1994)
13. U. Schlarb, M. Wöhlecke, B. Gather, A. Reichert, K. Betzler, T. Volk, N. Rubinina: Opt. Mater. (Amsterdam) **4**, 791 (1995)
14. U. Schlarb, A. Reichert, K. Betzler, M. Wöhlecke, B. Gather, T. Volk, N. Rubinina: Rad. Eff. Defects Solids **136**, 1029 (1995)
15. K. Kasemir, K. Betzler, B. Matzas, B. Tiegel, M. Wöhlecke, N. Rubinina, T. Volk: Phys. Status Solidi A **166**, R7 (1998)
16. K. Kasemir, K. Betzler, B. Matzas, B. Tiegel, T. Wahlbrink, M. Wöhlecke, B. Gather, N. Rubinina, T. Volk: J. Appl. Phys. **84**, 5191 (1998)
17. D. Xue, S. Zhang: Physica B **262**, 78 (1999)
18. I.D. Brown: Acta Cryst. B **48**, 553 (1992)
19. V.S. Urusov, I.P. Orlov: Crystallography Reports **44**, 686 (1999)
20. D.A. Kleinmen: Phys. Rev. **126**, 1977 (1962)
21. J.C. Phillips: Rev. Mod. Phys. **42**, 317 (1970)
22. J.A. van Vechten: Phys. Rev. **182**, 891 (1969)
23. B.F. Levine: Phys. Rev. B **7**, 2591 (1973)
24. D. Xue, S. Zhang: J. Phys. Condens. Matter **9**, 7515 (1997)
25. H. Neumann: Cryst. Res. Technol. **24**, 815 (1989)
26. J.M. Merino, R. Diaz, M. Leon: Phys. Rev. B **61**, 10211 (2000)
27. B.F. Levine: J. Chem. Phys. **59**, 1463 (1973)
28. B.F. Levine: Phys. Rev. B **7**, 2600 (1973)
29. S.C. Abrahams, P. Marsh: Acta Cryst. B **42**, 61 (1986)
30. Y. Ohkubo, Y. Murakami, T. Saito, A. Yokoyama, S. Uehara, S. Shibata, Y. Kawase: Phys. Rev. B **60**, 11963 (1999)
31. Y. Furukawa, K. Kitamura, S. Takekawa, K. Niwa, Y. Yajima, N. Iyi, I. Mnushkina, P. Guggenheim, J.M. Martin: J. Cryst. Growth **211**, 230 (2000)
32. H. Donnerberg, S.M. Tomlinson, C.R.A. Catlow, O.F. Schirmer: Phys. Rev. B **44**, 4877 (1991)
33. N. Iyi, K. Kitamura, F. Izumi, J.K. Yamamoto, T. Hayashi, H. Asano, S. Kimura: J. Solid State Chem. **101**, 340 (1992)
34. D. Xue, K. Betzler, H. Hesse: J. Phys. Condens. Matter **12**, 6245 (2000)
35. D. Xue, K. Betzler, H. Hesse: Opt. Commun. **182**, 167 (2000)
36. D. Xue, K. Betzler, H. Hesse: J. Appl. Phys. **89**, 849 (2001)
37. D.A. Roberts: IEEE J. Quantum Electron. **QE-28**, 2057 (1992)
38. R.C. Miller, W.A. Nordland, P.M. Bridenbaugh: J. Appl. Phys. **42**, 4145 (1971)
39. I. Shoji, T. Kondo, A. Kitamoto, M. Shirane, R. Ito: J. Opt. Soc. Am. B **14**, 2268 (1997)
40. N. Iyi, K. Kitamura, Y. Yajima, S. Kimura, Y. Furukawa, M. Sato: J. Solid State Chem. **118**, 148 (1995)